Protein Expression and Purification 186 (2021) 105918

Contents lists available at ScienceDirect

Protein Expression and Purification

journal homepage: www.elsevier.com/locate/yprep

Optimized expression and purification of a soluble BMP2 variant based on in-silico design

Tobias Heinks [a,*,1], Anette Hettwer [a,b,1], Christian Hiepen [c], Christoph Weise [c], Marcel Gorka [a], Petra Knaus [c], Thomas D. Mueller [b], Angelika Loidl-Stahlhofen [a]

[a] Westfälische Hochschule Recklinghausen, 45665, Recklinghausen, Germany
[b] Universität Würzburg, Department for Molecular Plant Physiology and Biophysics - Botany I, Julius-von-Sachs Institute, 97082, Würzburg, Germany
[c] Freie Universität Berlin, Institute of Chemistry and Biochemistry, 14195, Berlin, Germany

ARTICLE INFO

Keywords:
Bone morphogenetic protein 2
Aggregation-prone
In-silico-design
Hydrophilicity enhanced hBMP2 variant
E. coli SHuffle® T7
pH-shift elution

ABSTRACT

Bone morphogenetic protein 2 (BMP2[1]) is a highly interesting therapeutic growth factor due to its strong osteogenic/osteoinductive potential. However, its pronounced aggregation tendency renders recombinant and soluble production troublesome and complex. While prokaryotic expression systems can provide BMP2 in large amounts, the typically insoluble protein requires complex denaturation-renaturation procedures with medically hazardous reagents to obtain natively folded homodimeric BMP2. Based on a detailed aggregation analysis of wildtype BMP2, we designed a hydrophilic variant of BMP2 additionally containing an improved heparin binding site (BMP2-2Hep-7M). Consecutive optimization of BMP2-2Hep-7M expression and purification enabled production of soluble dimeric BMP2-2Hep-7M in high yield in *E. coli*. This was achieved by a) increasing protein hydrophilicity via introducing seven point mutations within aggregation hot spots of wildtype BMP2 and a longer N-terminus resulting in higher affinity for heparin, b) by employing *E. coli* strain SHuffle® T7, which enables the structurally essential disulfide-bond formation in BMP2 in the cytoplasm, c) by using BMP2 variant characteristic soluble expression conditions and application of L-arginine as solubility enhancer. The BMP2 variant BMP2-2Hep-7M shows strongly attenuated although not completely eliminated aggregation tendency.

1. Introduction

Autoinduction of bone growth was described in 1965 [1] and further explored in following years. In 1979 Urist et al. published a group of proteins that directly affected bone growth, which were named bone morphogenetic proteins (BMPs) [2–5]. First, BMPs were only classified as osteogenic growth factors (eponymous for their name) – concluding recruiting and proliferation of monocytes and mesenchymal cells, and inducing angiogenesis and differentiation to osteoblasts [6,7]. In subsequent studies, their activity-spectrum was extended and functionalities affecting the whole organism were identified, as for example regulating myogenesis [8], embryogenesis [9] and neural development [10]. This broad functionality is further highlighted by suggesting the acronym BMP to be interpreted as body morphogenetic proteins [11,12].

Within the transforming growth factor β family BMPs with 18–20 members form the largest subgroup [7,13]. The BMP subgroup can be further subdivided into the phylogenetically related BMP2/4, BMP3/3B, BMP5/6/7/8/8B, BMP9/10, BMP12/13/14, BMP11, BMP15/16 groups [7,9,14]. Among these, BMP2 is one of the most frequently studied BMPs and has gained high therapeutic interest for application in bone regeneration and healing. Indeed in 2002 BMP2 was approved by the FDA as a medical product [15] and is commercially available as InductOs® (European sector) or as Infuse® Bone Graft (USA sector) [16,17]. In both products, BMP2 is applied via a BMP2-soaked collagen sponge, which is implanted at the site of action. BMP2-soaked collagen sponges were employed in several medical fields (repair of tibial fractures [18], healing critical size defects [19] or spinal fusions [20]) where it could

Abbreviations: BMP2, bone morphogenetic protein 2; TGFβ, transforming growth factor ß; PSIPRED, PSI-blast based secondary structure PREDiction; HSA, Hot Spot Area; DLS, dynamic light scattering; R_h, hydrodynamic radius; FDA, U.S. Food and Drug Administration; preproBMP2, complete preproprotein wt-BMP2 (396 AA; NCBI, **NP_001191.1**).

* Corresponding author. Universität Bielefeld, Faculty for Chemistry, Biochemistry I, 33615, Bielefeld, Germany.
E-mail address: Tobias.Heinks@uni-bielefeld.de (T. Heinks).

[1] contributed equally to the work.

https://doi.org/10.1016/j.pep.2021.105918
Received 22 September 2020; Received in revised form 11 April 2021; Accepted 20 May 2021
Available online 24 May 2021
1046-5928/© 2021 Elsevier Inc. All rights reserved.

show clear medical benefits: shortened hospitalization and lower hospital-related costs [21,22]. However for the desired therapeutic effect BMP2 is used at quite high supra-physiological doses – while under physiological conditions ng-amounts are observed, in therapeutic application (e.g. InductOS®/Infuse® Bone Graft) high μg to mg amounts are implanted [23]– thereby increasing the risk of unwanted side effects either due to excessive inflammatory processes or diffusion of the protein from its site of implantation thereby causing formation of ectopic bone [24].

Human BMP2 (hBMP2) underlies a complex biological processing. The N-terminal signal peptide (23 amino acids, AA) gets cleaved off during the secretion process leaving a rather large dimeric proprotein consisting of 2x396 AAs. The proprotein is subsequently processed by metalloproteases of the furin family to remove the N-terminal propeptide. The remaining 2x114 residues yield the mature C-terminal dimeric BMP2 protein, which contains the highly characteristic cystine-knot motif and harbors all domains required for receptor binding and activation [25–28].

The cystine-knot motif formed by three intramolecular disulfide bonds between cysteine residues 296 and 361, Cys325 and Cys393, and between Cys329 and Cys395 (AA numbering according to the preproBMP2 sequence) provides BMP2 with a high physicochemical stability [29,30]. Together with covalent dimer formation via an intermolecular disulfide bridge involving the Cys360 residue in either monomer, BMP2 robustly withstands unfolding and retains its bioactivity even when exposed to harsh chemical conditions as reflected by Urist's BMP extracting procedures from bone utilizing strong acid and strongly denaturing chaotropic reagents such as urea and guanidinium hydrochloride. It is interesting to note that the cystine-knot motif is not unique to BMPs but present in all TGFβ family members as well as various BMP modulator proteins such as Noggin and members of the DAN family [31–33]. The overall structure of the BMP2-dimer can be described as the two monomers arranging like two inverse clasped hands. In this hand-like depiction the single long α-helix hereby forms the wrist, while the cystine-knot conforms to the palm and each of the two 2-stranded β-sheets are described as one finger [31,34]. Another characteristic property of BMP2 is its pronounced heparin binding which is possibly implemented through a stretch of mostly basic amino acids in the first 20 residues of the mature protein of which six are located in the very N-terminus of mature BMP2 (i.e. Lys285, Lys287, Arg289, Lys290, Arg291 and Lys293) and further two are placed just past the first Cys residue of the cystine-knot motif (i.e. Lys297 and Arg298) [36]. It is interesting to note that this basic N-terminus is not present in various other BMPs (as well as in TGFβs and activins) but only shared with BMP4 and might thus be involved in a differential tissue targeting of these two BMPs to ECM-rich cell surfaces [37]. The heparin-binding properties of BMP2 are moreover used to functionalize bioactive materials and to tune the biological activity of BMP2 with heparin-bound BMP2 having superior signaling activity over its heparin-unbound counterpart [38]. However, removal of the basic N-terminus of BMP2 did not fully abrogate heparin binding and thus additional positively charged patches in the cystine-knot containing part might also engage with heparin [35].

Dimer formation of BMP2 (as well as for other BMPs) is an essential prerequisite for receptor activation and BMP bioactivity. While usually homodimerization is assumed, BMP2 can also form heterodimers with certain other BMPs either by recombinant means but possibly also *in vivo*. BMP2 homo- and heterodimers differ only by receptor specificity and activity but seem not to affect the type of bone formation [6]. Receptor activation and initiation of BMP-signaling requires assembly of heterotetrameric receptor complexes consisting of so-called type I and type II receptors, which involves interactions between two different exposed epitopes (wrist and knuckle epitope) on the BMP2 surface to the membrane bound BMP-receptor type I and II with different affinities [39].

To enable biochemical studies different procedures were developed to obtain hBMP2 in larger quantities and with high purity. Initially BMPs were isolated from bones as mixtures, however this technique not only involved complex, time- and work-intensive methods (e.g. showed in Ref. [40]), but the extracted material in addition is allogenic and might thus present a health risk [41]. Furthermore, the yield and also biological activities of isolated BMP proteins were low (1–3 μg per kg bone [40,42,43]). Currently, medically applied and commercially produced rhBMP2 is expressed in CHO-cells. However, recombinant expression and high yield production of BMP2 in eucaryotic cells such as CHO cells [27] or Sf9 insect cells [44] proved to be challenging since the expression as preproprotein is absolutely required for proper rhBMP2 production. Additionally, eucaryotic expression systems harbor low up-scaling capacity, high production times and hence high total costs compared to procaryotic systems [45]. Furthermore, in eucaryotic systems high attention need to be paid to growth media due to sophisticated requirements of mammalian cells, to high contamination risks and to ethical criteria when producing biopharmaceutical proteins [45–49]. Comparative production of the humanized antibody fragment ACT017 revealed a slightly higher heterogeneity when using *E. coli* but most of all a notable reduced culture time and lowered costs [50]. A further limiting step in eucaryotic BMP2-production could be the proteolytic processing of the proprotein by metalloproteases of the furin family to release the mature C-terminal growth factor if furin proteases are not overexpressed simultaneously. As BMP2 does not require post-translational modifications such as glycosylation for activity [36] recombinant production in *E. coli* seems highly attractive since *E. coli*-derived rhBMP2 shows appropriate properties (e.g. nanomolar solubility in aqueous solutions and thermal stability in acidic buffers) and biological activity (e.g. shown in Refs. [51–53]). However, the requirement of disulfide bond formation to establish the cystine-knot as well as the presence of large hydrophobic surface patches in the C-terminal growth factor domain result in BMP2 being expressed usually insoluble into bacterial protein aggregates termed inclusion bodies. Hence production of BMP2 from bacteria comprises an *in vitro* oxidative refolding step [54], which not only is time- and cost-intensive but involves the usage of hazardous substances (e.g. DTT, guanidinium chloride, urea) that can be incompatible with or at least requires additional work to obtain approval as therapeutic substance through medical agencies such as FDA and EMA [36,43,55].

In this work we therefore aimed to produce a biofunctional BMP2 with enhanced heparin binding and attenuated aggregation tendency, utilizing a soluble high-yield expression system combined with a simple, time- and cost-saving purification technique avoiding harmful chemistry. This allows an economic and inexpensive direct production of soluble BMP2.

2. Materials and methods

2.1. Annotation

All prokaryotic expression systems start translation with f-Formyl-Met, which is normally cleaved later on. However, this is not the case, when the aminoterminal AA of a protein is larger than valine [56]. Due to cloning procedure the construct we used as mature BMP2 (wt-BMP2*) has an artificially added alanine upstream the native glutamine, whereas our new BMP2-mutant (BMP2-2Hep-7M) starts with the native glutamine as first AA downstream the starting methionine. Following protein expression in *E. coli* methionine is cleaved in wt-BMP2* (since alanine is smaller than valine) and not cleaved in the mutant (since glutamine is bigger than valine). This leads to wt-BMP2* starting with AQ and in conclusion 115 amino acids (annotation shift +1) [36] and to BMP2-2Hep-7M starting with MQ. Additionally, the amino acid positions according to the preproBMP2 sequence are indicated.

2.2. In silico design of BMP2-2Hep-7M

The human BMP2 protein sequence was analyzed for aggregation hot spots using the *AggreScan* algorithm [57]. Seven hydrophilizing amino acid exchanges were set within 6 detected aggregation hot spots, while the BMP2 receptor type I and type II interacting positions [39,58] were preserved. In addition, the basic N-terminus of BMP2 was modified to enhance its heparin binding capacity [35,36,59]. This was achieved by introducing multiple copies of basic motifs, e.g. KHK and KR, similar to the approach published by Wuerzler *et al.* [60] (see also [61]). Subsequently, the new construct BMP2-2Hep-7M was reassessed with *AggreScan* thereby confirming the almost complete absence of aggregation hot spots. To predict probable secondary structures the PSI-blast based secondary structure prediction tool (*PSIPRED*) was applied [62].

2.3. Cloning of BMP2-2Hep-7M-gene

A synthetic gene encoding BMP2-2Hep-7M with an optimized codon-usage for expression in *E. coli* was purchased from Eurofins Genomics, Ebersberg Germany. Restriction sites of *Nde*I and XhoI were inserted at the 5′ and 3′-ends of the bmp2 gene to allow directed cloning into the expression vector pET32a (Novagen). The cDNA sequence of the resulting plasmid (pBMP2-2Hep-7M) was confirmed by DNA-sequencing (Eurofins Genomics, Ebersberg, Germany).

2.4. Protein expression

2.4.1. Optimization of BMP2-2Hep-7M expression

The BMP2-2Hep-7M monomer comprises 122 amino acids corresponding to a molecular weight of 13965.9 Da. In order to determine an efficient expression host four different *E. coli* strains, i.e. BL21 (DE3), Origami™ B (DE3), SHuffle® T7, and ArcticExpress™ (DE3), were transformed with pBMP2-2Hep-7M. Positive clones were obtained on LB-agar plates containing 100 μg/ml ampicillin (plus additional gentamycin (20 μg/ml) when using *E. coli* ArcticExpress™ (DE3)) and were used to generate glycerol stocks for inoculating overnight precultures.

Expression cultures were incubated at 37 °C to an optical density at 600 nm of 0.6, then protein expression was induced by addition of Isopropyl ß-D-1-thiogalactopyranoside (IPTG; 0.5 or 1.0 mM). To test the influence of temperature of protein production, expression was performed at different temperatures (13 °C for ArcticExpress™ (DE3), 20 and 30 °C for all strains and additionally at 34 and 37 °C for SHuffle® T7). Protein expression lasted 24 h employing LB medium containing 100 μg/ml ampicillin (plus additional gentamycin (20 μg/ml) when using *E. coli* ArcticExpress™ (DE3)). Protein production was analyzed by SDS-PAGE using samples for whole cell lysates and corresponding ones separated for soluble and insoluble fraction after sonication and centrifugation. To monitor the time course of expression samples were taken at 0, 1, 2, 3, 4.5, 6 and 24 h after addition of IPTG.

2.5. Final expression

After optimization preparative expression of BMP2-2Hep-7M was performed with pBMP2-2Hep-7M transformed *E. coli* SHuffle® T7 in LB-medium at 34 °C. Protein expression was induced at an optical density at 600 nm of 0.6 by addition of 1 mM IPTG. After 6 h cells were harvested by centrifugation for 20 min at 15.300×*g* and 4 °C (Avanti JXN-26 centrifuge, rotor JA-14). Cell pellets were stored at −20 °C.

2.6. Heparin-sepharose chromatography

2.6.1. Purification studies/analysis

After thawing, cells were resuspended in different resuspension buffers (Table 2) (25 ml/g cells wet weight) and lysed by sonication at 10 × 30 s bursts (Sonoplus HD 2200.2, sonotrode VS70T, Bandelin). The lysate was supplemented with different solubility-enhancing additives (Table 2), incubated for 2 h on ice and centrifugated at 48.300×*g* for 10 min at 4 °C (Avanti JXN-26 centrifuge, rotor JA-25.50). Heparin resin (5 ml HiTrap Heparin HP column; GE Healthcare, Äkta-FPLC system) was used as initial purification step as both cation exchange and affinity. For optimization of the purification conditions different buffers for washing and protein elution were tested (Table 3). Protein elution was achieved using a linear gradient moving to different elution buffer conditions in six column volumes. Protein-containing elution fractions were analyzed by Tricine-SDS-PAGE and dynamic light scattering (DLS) measurements.

Table 1
Protein expression analysis for BMP2-2Hep-7M. Expression was done in different *E. coli* hosts (ArcticExpress™ (DE3), BL21(DE3), Origami™ B (DE3), SHuffle® T7), at various expression temperatures induced with different concentrations of IPTG. Expression efficiency is shown as no (−) and low (±) to high ($+_n$) intensities in whole protein (first position) vs. soluble protein (second position).

	whole protein/soluble protein					
	0.5 mM IPTG			1.0 mM IPTG		
	Expression time [hrs]			Expression time [hrs]		
***E. coli* strain**	3	5	24	3	5	24
	13 °C			13 °C		
ArcticExpress™ (DE3)	−/−	−/−	−/−	−/−	−/−	−/−
	20 °C			20 °C		
BL21 (DE3)	−/−	−/−	−/−	−/−	−/−	−/−
Origami™ B (DE3)	−/−	−/−	−/−	−/−	−/−	−/−
SHuffle® T7	−/−	−/−	−/−	±/±	±/±	+/−
	30 °C			30 °C		
BL21 (DE3)	−/−	−/−	−/−	−/−	−/−	−/−
Origami™ B (DE3)	+/+	+/+	+/−	++/++	++/++	+/±
SHuffle® T7	+/+	+/+	+/−	++/++	++/++	+/±

Table 2
Heparin-Sepharose purification analysis for BMP2-2Hep-7M. The purification was done with various additives after cell lysis and different chromatography buffers. *wash buffer without additives; **equal buffer conditions compared to lysate; ***equal results when using L-arginine (0.5 M) in wash buffer or not; is = insoluble; s = soluble; ft = flow through; nd = not determined; (-/±/$+_n$) = indicating no/low/high staining intensities for BMP2-2Hep-7M dimer.

	additives in lysate*			pH		
	NaPi-buffer pH 7.4			NaPi-buffer		
fraction	w/o	10% Glycerol	0.5 M L-arginine	6.0	7.4	9.1
is	++	++	+	nd	nd	nd
s	++	+	++	++	+	+
ft	++	+	–	+	+	+
				Additives in lysate/wash buffer		
	pH **5.3**			**Tris** pH **5.3**		
fraction	NaPi	Tris		0.5 M L-arginine ***	1 M L-arginine	0.5 M L- arginine 6 M urea
is	nd	nd		±	±	±
s	++	++		+++	++	++
ft**	+	–		–	++	±

2.6.2. Final purification

For preparative preparations native BMP2-2Hep-7M dimer was obtained from lysing the cells by sonication using 50 mM Tris-HCl pH 5.3 (25 ml/g cell wet weight). The lysate was supplemented with 0.5 M L-arginine and the protein solution was incubated for 2 h on ice. The

Table 3
A: Relative estimation of BMP2-2Hep-7M protein expression after heparin-Sepharose chromatography evaluated by analytical SDS-PAGE and DLS analysis. B: Composition and conditions of different elution buffer systems and additives evaluated. n = not detectable; R_h: hydrodynamic radius, * = according to R_h of wt-BMP2* dimer.

A)	No. of elution buffer					
	1	2	3	4	5	6
Elution fractions						
E. coli proteins	+++	+	++	+	+++	++
BMP2-2Hep-7M	+	+		+		
$(BMP2\text{-}2Hep\text{-}7M)_2$	–	+	+	++	++	+++
high Rh (>10 nm)/%	100	100	100	100	n	8.4
low Rh (4–8 nm*)/%	0	0	0	0	n	91.6

B) **No. of elution buffer**	pH **50 mM Tris**	**Additives/M** **L-arginine**	**NaCl**	**urea**
1	5.3	w/o	2	w/o
2	5.3	w/o	2	6
3	5.3	0.5	2	6
4	5.3	1.0	1	w/o
5	7.4	0.5	0.5	w/o
6	8.8	0.5	0.5	w/o

protein was purified by cation exchange and affinity chromatography using a 5 ml HiTrap Heparin HP column (GE Healthcare) and applying a linear gradient from 50 mM Tris-HCl, pH 5.3, 0.5 M L-arginine to 50 mM Tris-HCl pH 8.8, 0.5 M NaCl, 0.5 M L-arginine in six column volumes. The pH of the resuspension and application onto the column (Tris-HCl pH 5.3) was controlled and maintained constantly.

2.6.3. Size exclusion chromatography

BMP2-2Hep-7M-containing fractions were pooled and further purified by size exclusion chromatography (HiPrep 16/60 Sephacryl S-100 HR column; GE Healthcare) performed on an Äkta FPLC-system (flow-rate of 0.4 ml/min) using 50 mM Tris-HCl pH 8.8, 0.5 M NaCl, 0.5 M L-arginine.

2.7. Protein characterization

2.7.1. DLS measurements

DLS measurements were done on a Zetasizer Nano (Malvern Panalytical) at 20 °C, number of experiments n = 6 (Zetasizer was instructed to repeat scanning for at least 10 times before displaying the average result of an experiment).

2.7.2. SDS-PAGE

Protein purity was analyzed via TRIS-Tricine-SDS-PAGE [63] under non-reducing conditions to analyze disulfide bond-mediated dimer formation. Proteins were visualized by colloidal coomassie staining [64]. PageRuler Prestained Protein Ladder (#26616, Thermo Fisher Scientific) or Color Prestained Protein Standard (#P7712, New England Biolabs) was used as protein molecular weight standard.

2.7.3. Protein concentration

Protein concentrations were estimated using the absorbance at 280 nm in a standard spectrophotometer (Biospectrometer® Eppendorf AG).

2.7.4. MALDI-TOF mass spectrometry

Purified BMP2-2Hep-7M protein was examined by matrix-assisted laser desorption ionization/time-of-flight mass spectrometry (MALDI-TOF-MS) on an Ultraflex-II TOF/TOF instrument (Bruker Daltonics) equipped with a 200 Hz solid-state Smart beam™ laser. Sequence information was obtained by in-source decay (ISD) generating N-terminal c and C-terminal (z+2) sequence ions. The samples were applied onto the MALDI target using the dried-droplet method with 1,5-diaminonaphthalene (1,5-DAN) as matrix (20 mg/ml 1,5-DAN in 50% acetonitrile/0.1% trifluoroacetic acid). Spectra were recorded in the positive reflector mode (RP PepMix) in the mass range 600–4000. Sequence assignment was done manually.

3. Results

3.1. Construction of the BMP2-2Hep-7M variant

Bone morphogenetic protein 2 is a highly aggregation-prone protein. Its recombinant expression in *E. coli* usually results in formation of protein aggregates termed inclusion bodies present in the bacterial cytoplasm, which then demands for complex and time-consuming renaturation steps to yield pure natively folded protein. Removal of renaturation reagents that can be harmful to biological experiments and for *in vivo* use require excessive dialysis and an effective (multistep) purification [31,36,53].

To identify aggregation hot spots in BMP2* we applied *AggreScan* [57], an algorithm that predicts aggregation-prone segments in protein sequences *in silico*. Six aggregation hot spots were identified in the mature domain of BMP2* (maximum in HSA: 4.233). We then replaced hydrophobic amino acid residues within these six regions that are not involved in receptor binding [39,58] with hydrophilic amino acids. The designed mutants were again analyzed by *AggreScan* revealing that all aggregation hot spots were removed leaving only one remaining aggregation hot spot of moderate intensity (Peak = 1.837) caused by alanine 35 (corresponding to alanine 316 in the completely annotated sequence of BMP2; NCBI: NP_001191.1) (Fig. 1). In wildtype BMP2 this residue was shown to be indispensable for type II receptor binding and hence bioactivity [39,58].

In order to facilitate purification of soluble BMP2 from the bacterial cytoplasm, heparin-binding of BMP2, a feature of the wildtype growth factor, was further enhanced by inserting additional basic triplet motifs at the N-terminus of the protein [36]. Besides, increasing the hydrophilic character of the BMP2 N-terminus and simultaneously easing purification by heparin affinity or ion exchange chromatography enhanced heparin binding was found to modulate *in vitro* and *in vivo* bioactivity of the osteoinductive BMP2, which might be beneficial for later application and further functionalization of our designer BMP2 variant [36,38,60,65,66].

Sequence comparison of wt-BMP2* and the new BMP2 variant (BMP2-2Hep-7M) with *PSIPRED* [67–69], an open source fold recognition tool, revealed high secondary structure homology (Fig. 2). Only the short β-sheet at position 108 to 111 (corresponding to AA389 to AA392 of preproBMP2) is missing in the variant which is expected to not interfere with receptor binding. The wrist forming α-helix of BMP2* is predicted for the positions 60–70 (corresponding to AA341 to AA351 of preproBMP2) in the wildtype protein with high confidence and with the same certainty for position 68–78 (corresponding to $AA341_{+8}$ to $AA351_{+8}$ of preproBMP2) in the BMP2-2Hep-7M variant. Doubling of the heparin binding site leads to a longer N-terminal tail in the variant: however, this is partly compensated by a new N-terminal α-helical structure formed by 12 amino acids (position 3–15 (corresponding to $AA283_{+1}$ to $AA288_{+8}$ of preproBMP2)) and predicted with high confidence.

3.2. Production of BMP2-2Hep-7M

Recombinant expression of BMP2-2Hep-7M protein was tested under different conditions employing a screen of different expression strains, altering expression temperature, inducer (IPTG) concentration and expression length. Results were studied by comparative SDS-PAGE analysis. Protein production in different *E. coli* strains before (0 h) and after (1, 2, 3, 4.5/5, 6 and 24 h) induction of protein expression and the soluble/insoluble fractions after sonication of probes at given timepoints

A

wt-BMP2*

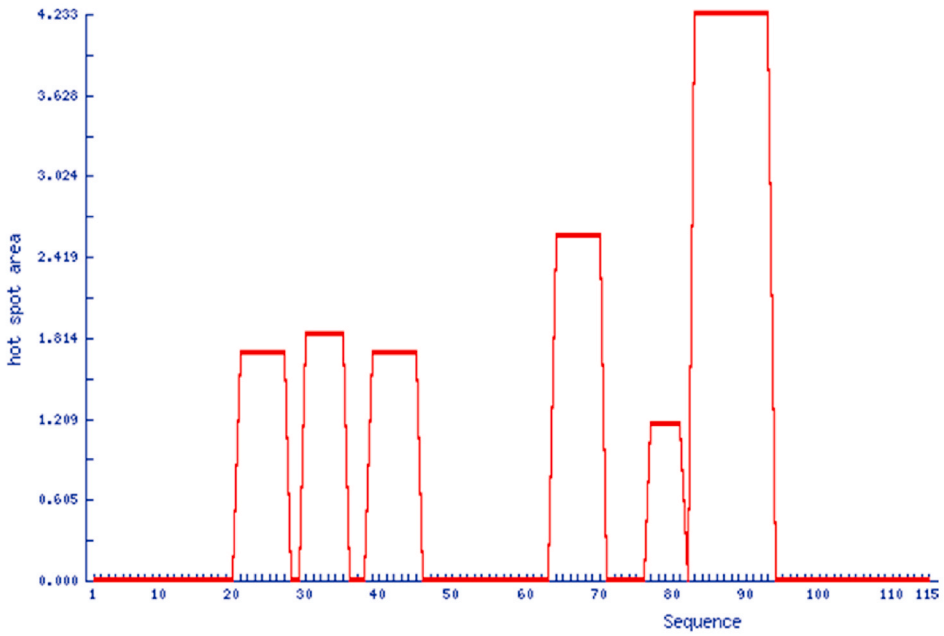

BMP2-2Hep-7M

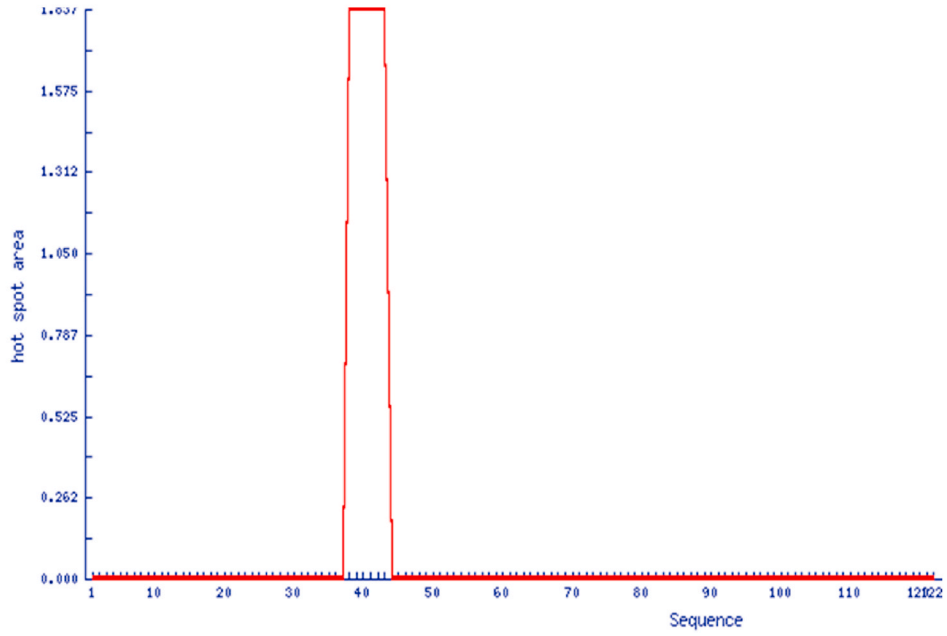

Fig. 1. A: AggreScan-analysis of wildtype BMP2* and BMP2-2Hep-7M; B: Amino acid sequence alignment of wildtype BMP2* (upper) and BMP2-2Hep-7M (lower). Positions with amino acid residues exchanged for more hydrophilic amino acid types (6 amino acids) are indicated with bold red letters, additional basic amino acids at the N-terminus (AKHKQRKR) are highlighted in green, the deletion at position 107 in wildtype BMP2* is marked with a red arrow, regions identified as aggregation hot spots are highlighted in grey (low/medium HSA < 2) or yellow (strong HSA>2). Amino acids are numbered according to the biologically cleaved mature BMP2*(1–115) corresponding to AA282 to AA396 of the completely annotated sequence of BMP2 (NCBI: **NP_001191.1**), while for BMP2-2Hep-7M amino acids ($1–115_{+7}$) were aligned to the mature wt-BMP2 sequence with indices regarding the 8 insertions and 1 deletion.

B

```
wt-BMP2*          1   AQ              AKHKQRKR LKSSCKRHPL YVDFSDVGWN DWIVAPPGYH  40
BMP2-2Hep-7M      1   MQ AKHKQRKR AKHKQRKR LKSSCKRHPL YVDYSDVGWN DWIVAPPGYH  40+8

wt-BMP2*         41   AFYCHGECPF PLADHLNSTN HAIVQTLVNS VNSKIPKACC VPTELSAISM  90
BMP2-2Hep-7M  41-8   NFYCHGECPF PLADHLNSTN HAITQTLVNS VNSKIPKACC TPTELSASSQ  90-8

wt-BMP2*         91   LYLDENEKVV LKNYQDMVVE GCGCR  115
BMP2-2Hep-7M  91-8   LYLDENEKVV LKNYQD---VVE GCGCR  115+7
                                        ⬆
```

Fig. 1. (*continued*).

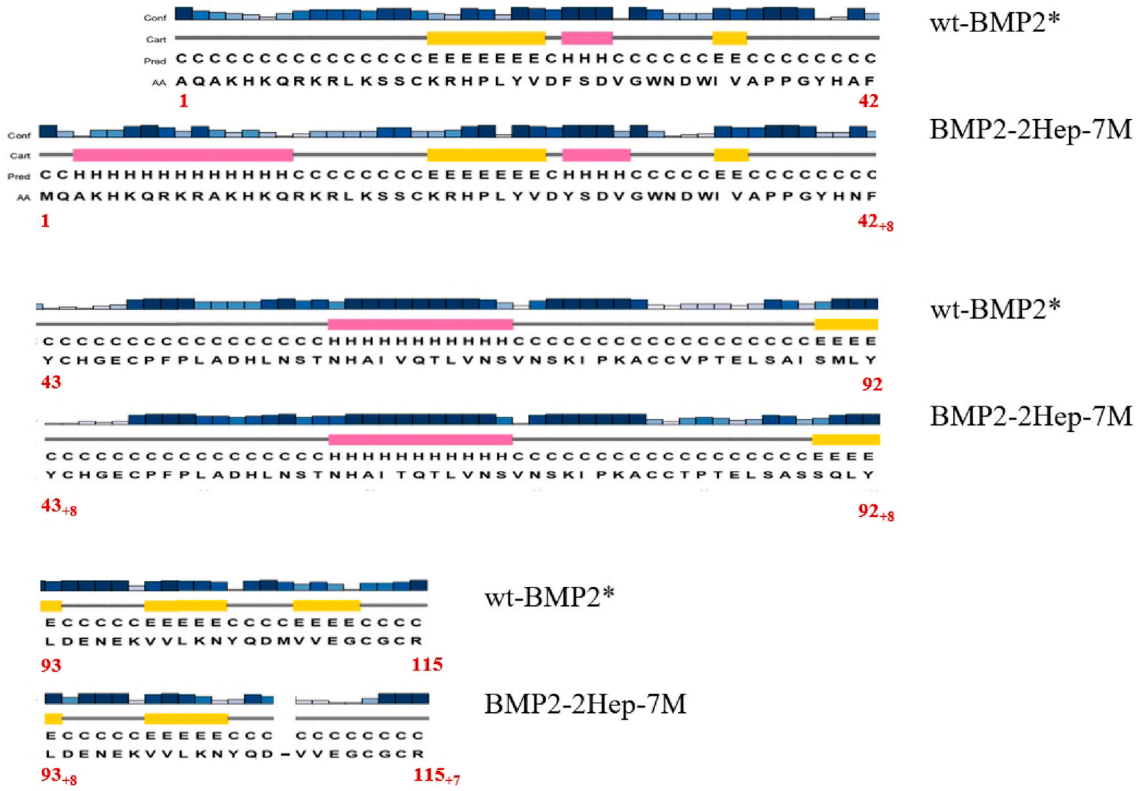

Fig. 2. Secondary structure prediction of wt-BMP2* (upper) and BMP2-2Hep-7M (lower) analyzed by PSIPRED. Pink bars mark α-helical segments, yellow bars indicate β-strands. Intensity of the blue stacks above the sequence refers to confidence interval of prediction. Amino acids 1 to 115 correspond to the mature wt-BMP2* protein (corresponding to AA282 to AA396 of preproBMP2) and amino acid annotation for BMP2-2Hep-7M (1–115_{+7}) is based on this mature wt-BMP2* sequence completed with indices regarding the 8 insertions and 1 deletion.

(3, 5, 24 h) were evaluated. Table 1 summarizes the expression data with staining intensity for BMP2-2Hep-7M monomer protein indicated with (±or -) for low or no expression and $(+)_n$ for stronger target protein expression as analyzed from whole cell lysates (whole protein, first position) and for the analysis of the soluble and insoluble fraction (soluble protein, second position).

3.3. Protein expression analysis for BMP2-2Hep-7M

We could not detect any BMP2-2Hep-7M expression in the *E. coli* strain Artic Express™ (DE3) albeit low expression temperatures and the co-expression of bacterial chaperones (a characteristic of this particular *E. coli* expression strain) should facilitate proper folding of aggregation-prone proteins [70,71]. The strongest expression of soluble BMP2-2Hep-7M monomer was found for the *E. coli* strains Origami™ B (DE3) and SHuffle® T7 at 30 °C and using relatively high IPTG concentrations of 1 mM, while expression test performed at lower temperatures and lower IPTG concentrations indicated lower or even no soluble target protein expression, which seems counterintuitive at first sight. Expression tests in *E. coli* BL21 (DE3) showed expression neither of soluble nor of insoluble target protein monomer. Unfortunately, a significant formation of BMP2 dimer could not be detected for the above-listed *E. coli* strains when analyzed by non-reducing Tricine-SDS-PAGE. However, using *E. coli* SHuffle® T7 as expression host and using 34 °C as expression temperature, a BMP2-2Hep-7M dimer-band appeared in whole cell lysate probes under non-reducing conditions in a time-dependent manner. The protein band with a correct apparent molecular weight was confirmed as the anticipated BMP2 dimer by

SDS-PAGE under reducing conditions, which showed decreased staining intensity for the dimer, while the staining intensity for the monomer increased (Fig. 3). Further raising the expression temperature to 37 °C however strongly decreased the yield of BMP2 dimer (less to no dimer-band in SDS-gel; data not shown).

Comparative expression of BMP2-2Hep-7M vs. wt-BMP2* in *E. coli* SHuffle® T7 clearly showed that only BMP2-2Hep-7M can be produced in high yield as soluble protein whereas wt-BMP2* leads to insoluble protein aggregates (Fig. 4).

3.4. Mass-spectrometric analysis of the BMP2-2Hep-7M variant

In order to ascertain that the correct full-length BMP2-2Hep-7M is indeed expressed, prominent protein bands on dimer and monomer height (see Figs. 3, 6 and 7) were excised from gel and further examined by mass spectrometry. As shown in Fig. 5, N-terminal c ions (c8 to c25) as well as C-terminal (z+2) ions (z18-z30) were detected in MALDI in-source decay analysis. The mass values are in accordance with the theoretical values calculated from the sequence given in Fig. 1B, and one can conclude that both termini are correctly expressed, including the inserted N-terminal heparin-binding cassette. Additionally, the mass of the intact protein was determined by ESI-MS (data not shown) and the experimental values corresponded to the theoretical masses for monomer and dimer, respectively, within the experimental error. Collectively, the mass spectrometry data document beyond reasonable doubt that full-length BMP2-2Hep-7M including the N-terminal methionine is expressed in *E. coli* SHuffle® T7.

3.5. Purification of BMP2-2Hep-7M

An optimized purification method for soluble BMP2-2Hep-7M was established. First, different solubility enhancing additives were added to the cell lysate in order to increase the yield of soluble BMP2-2Hep-7M. Then different protein chromatography setups on heparin-Sepharose were tested to optimize the yield of pure BMP2 in dimeric form (see Table 2).

The results, i.e. expression yield of BMP2-2Hep-7M in the soluble and insoluble fractions, were evaluated on the basis of staining intensities in the subsequent SDS-PAGE analysis. The best purification conditions, i.e. high concentration of the BMP2 variant in the soluble fraction and low concentrations or absence in the insoluble fraction with no or low amounts of BMP2 protein in the flow-through fraction of the chromatography were obtained with lysate in Tris pH 5.3 supplemented with 0.5 M L-arginine. The following table summarizes the results, with (−) [no], (±) [low] and $(+)_n$ [high] indicating the staining intensities of BMP2-2Hep-7M dimer analyzed by non-reducing Tricine-SDS-PAGE.

3.6. Heparin-sepharose purification analysis for BMP2-2Hep-7M

The effects of different elution buffers and additives on purification

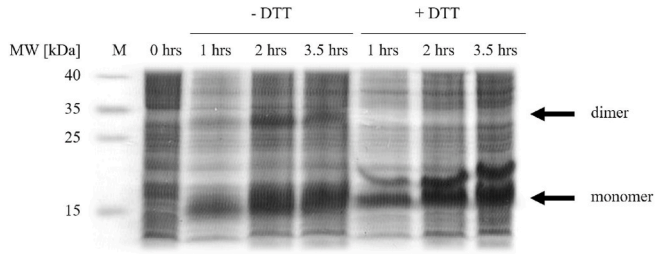

Fig. 3. Expression of recombinant BMP2-2Hep-7M in *E. coli* SHuffle® T7. Time course analysis of protein expression in whole cell lysates upon induction by 1 mM IPTG at 34 °C partially followed by DTT reduction [72] and non-reducing SDS-PAGE stained by Coomassie blue. Lane M: protein molecular weight standard.

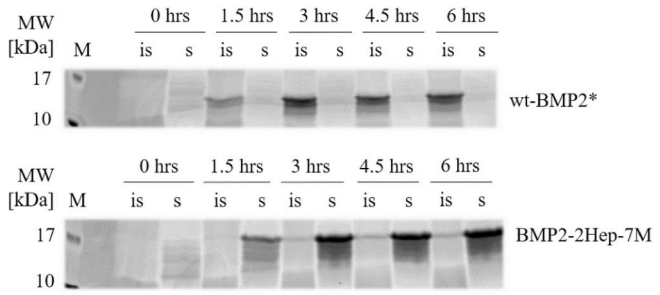

Fig. 4. Comparative expression of BMP2-2Hep-7M vs. wt-BMP2*. Time course analysis of soluble (s) and insoluble (is) fractions after sonication of comparative protein expression upon established expression conditions followed by reductive SDS-PAGE stained by Coomassie blue. Lane: protein molecular weight standard.

were further evaluated by DLS analysis to obtain insights on the oligomerization status of the BMP2 protein. Bioactive dimeric wildtype BMP2 has a rather low hydrodynamic radius (R_h) of 4–8 nm depending on buffer conditions and protein concentration (data not shown).

In contrast significantly higher high R_h values (>80 nm) indicate higher molecular weight aggregates. While avoiding formation of molecular aggregates is important, dimer formation for BMP2 is also essential as monomeric BMP2 is inactive. Thus, the presence and amount of BMP2 dimer was monitored throughout optimization of protein production and purification. From our optimization setup we found that only solution systems with a low pH/low salt concentration during application and buffers with high pH and low salt concentration for elution yielded BMP2-containing elution fractions, which comprised protein species with a small hydrodynamic radius (R_h) contaminated with large molecular weight BMP2 aggregates. At the same time these fractions contained large amounts of dimeric BMP2 while BMP2 monomer species were low as judged from SDS-PAGE analysis (Figs. 6 and 1s).

DLS analysis and SDS-PAGE are summarized in Table 3A: (−) [low/no] and $(+)_n$ [high] refer to the relative populations (in %) as determined by DLS and the staining intensities of the BMP2 protein bands in the SDS gel.

3.7. DLS and SDS-PAGE evaluation of BMP2-2Hep-7M yield after heparin-sepharose chromatography (different buffer compositions/conditions)

Our data show that using a single step cation exchange/affinity chromatography employing heparin-Sepharose was successful in a substantial enrichment of BMP2-2Hep-7M from most endogenous *E. coli* proteins. Elution fractions from this chromatography step that were highly enriched in dimeric BMP2-2Hep-7M were then further purified by gel filtration using a XK16/60 Sephacryl S-100 HR column (GE Healthcare). Size exclusion chromatography of BMP2 proteins derived from ion exchange elution fractions with a large hydrodynamic radius (R_h) revealed that these protein species were usually found in a single peak in the void volume and when analyzed by DLS again exhibit high R_h values. In analogy, when gel filtration was performed with ion exchange-purified fractions of BMP2 that exhibited small R_h values, no high-molecular weight aggregates (in the void volume) were found and monomeric and dimeric BMP2-2Hep-7M protein could be isolated.

After size exclusion chromatography, fractions enriched with BMP2-dimer protein were pooled, dialyzed against 1 mM HCl and freeze-dried. Fig. 6 presents the SDS-PAGE analysis of a BMP2-2Hep-7M purification. The established purification protocol yielded about 9–10 mg protein per liter expression volume.

Fig. 7 displays the final product of the established purification setup showing small contaminating amounts of residual *E. coli* proteins with a prominent dimeric BMP2-2Hep-7M band verified by mass spectrometry.

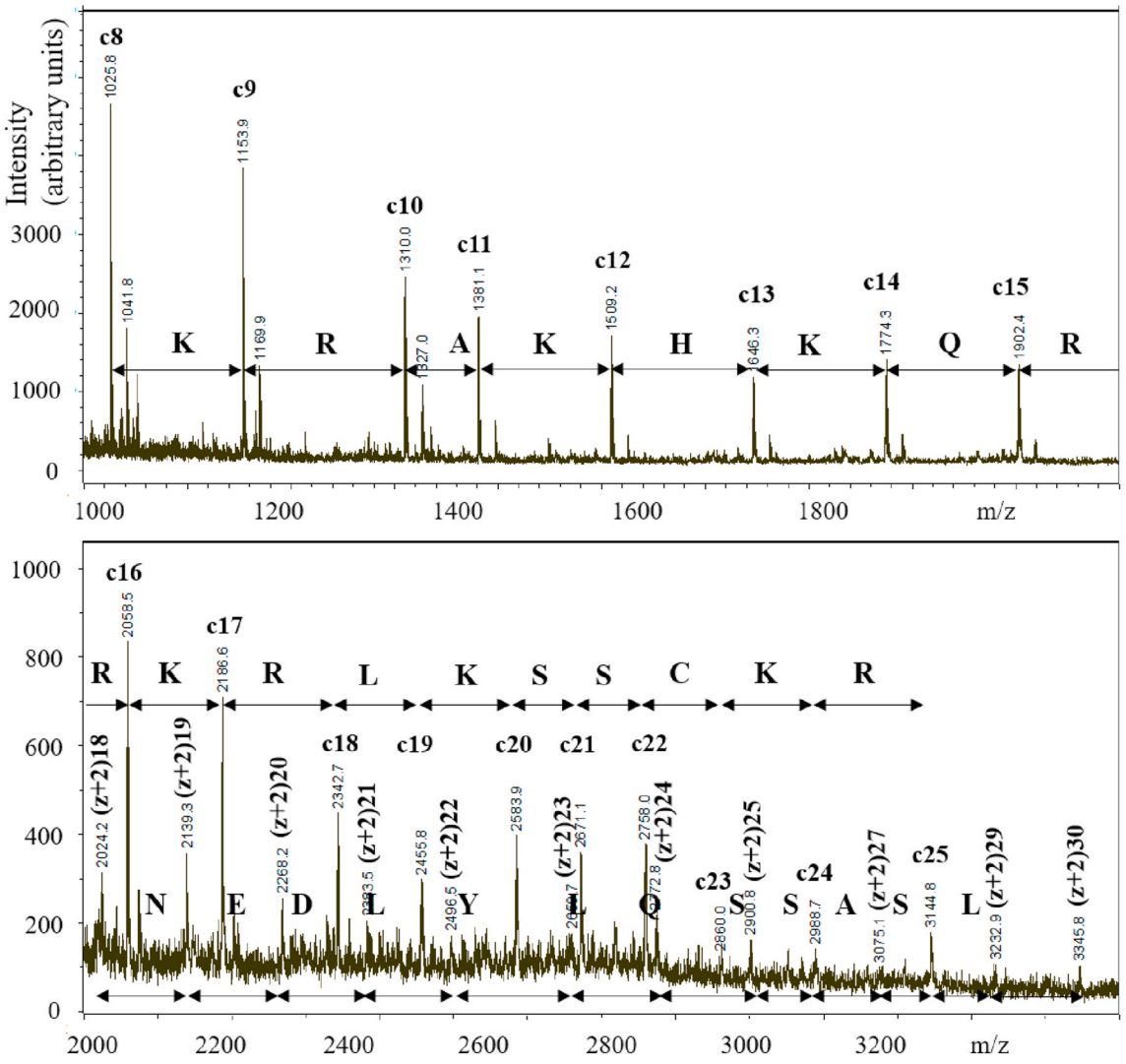

Fig. 5. Mass-spectrometric analysis of BMP2-2Hep-7M. In-source decay yields sequence ions (N-terminal c ions 8–25 and C-terminal (z+2) ions 18–30 in the mass range 1000–3500). The masses are in good agreement with the theoretical values (see supplemental data).

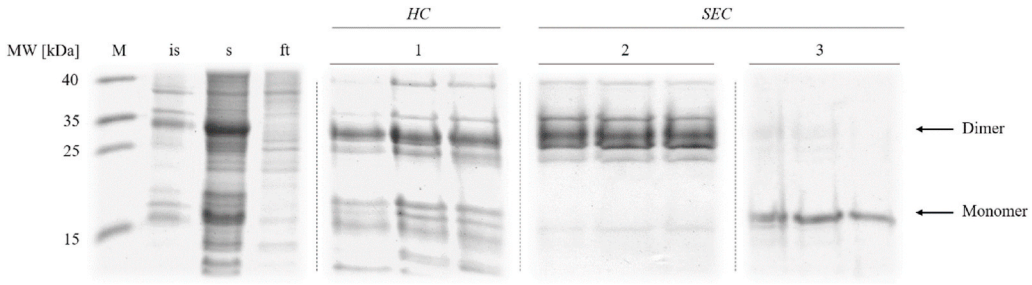

Fig. 6. Two-step purification of BMP2-2Hep-7M from *E. coli* SHuffle® T7 lysates employing heparin-Sepharose ion exchange chromatography (HC) and subsequent size exclusion chromatography (SEC). Protein fractions were analyzed using SDS-PAGE under non-reducing conditions, SDS-gels were stained with Coomassie blue (combined SDS gels are shown; separation of each gel is indicated by dotted lines). M: protein molecular weight standard; is/s = insoluble/soluble fraction; ft = flow through; *HC*-1: late elution fractions in ion exchange chromatography using heparin-Sepharose containing mainly BMP2 dimer; *SEC*-2: early elution fractions of size exclusion chromatography predominantly containing BMP2 dimer; *SEC*-3: late elution fractions comprising mainly monomeric BMP2.

Most of all, endogenous ribosomal proteins (i.e. S3, S4, L2, L15) and translation initiation factor IF-3 were co-purified. Minor contaminations result from low amounts of monomeric and oligomeric BMP2-2Hep-7M states.

4. Discussion

Producing therapeutic proteins in prokaryotic expression systems often presents a challenging task particularly when (human) post-translational modifications (e.g. glycosylation), properly folded proteins (e.g. requirement of disulfide bond formation) and defined oligomerization states are required for their function. These constraints also apply

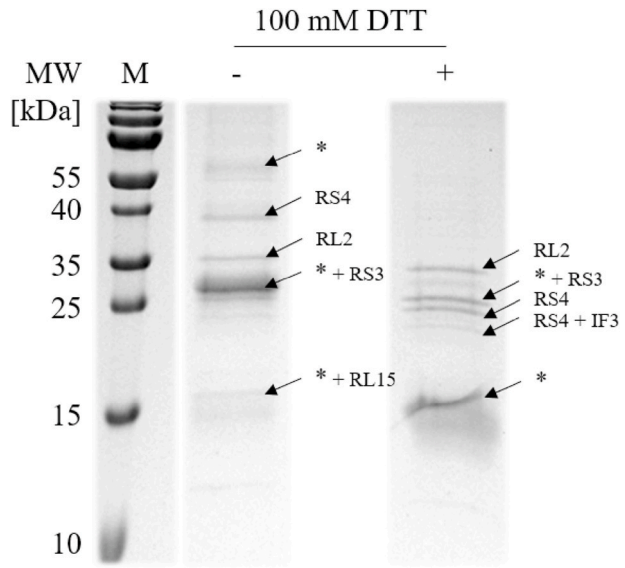

Fig. 7. Final product of established purification setup. Elution fractions after final purification was separated by reducing (100 mM DTT) and non-reducing SDS-PAGE and protein bands were verified by mass spectrometry. Lane M: protein molecular weight standard.

to the production of recombinant BMP2 a therapeutically valuable protein for application in e.g. human regenerative medicine such as bone repair. To exert bioactivity BMP2 requires a complex disulfide-bonded cystine-knot and the formation of its homodimeric architecture. While it can be efficiently expressed in *E. coli*, cystine-knot and dimer formation cannot be easily achieved in the prokaryotic expression system often resulting in the production of BMP2 as insoluble protein aggregates that are deposited in form of inclusion bodies in the bacterial cytoplasm. From these BMP2 must be extracted, processed via oxidative *in vitro* refolding to attain its dimer architecture comprising the cystine-knot and purified via a multistep procedure to remove inactive unwanted mono- and multimer species [43,54,55,73–77]. From this procedure a series of potential complications have to be considered: (a) refolding efficiency was shown to be a highly time-dependent and time-consuming step as refolding and particularly dimer formation seem to occur slowly (days to weeks), (b) multistep purification protocols strongly diminish target protein yield requiring larger amounts of starting material and (c) current refolding schemes comprise the usage of toxic/hazardous chemical reagents (e.g. urea/guanidinium hydrochloride, lithium sulfate, detergents CHAPS or CHES [36,43,55]) that must be efficiently removed if the target protein shall be used as a medical product for humans. All these issues make the current production processes time-consuming, costly or difficult for scale-up.

As an alternative production scheme, we designed a BMP2 variant (BMP2-2Hep-7M) that can be expressed as soluble protein in prokaryotes with an assured attenuated aggregation tendency compared to wt-BMP2* (see Fig. 4). Using the *in silico* tool *AggreScan*, the hydrophilicity of BMP2 was enhanced by introducing seven point mutations at residues not involved in BMP2-receptor binding. Analysis of the BMP2 variant BMP2-2Hep-7M by *AggreScan* revealed one remaining aggregation hot spot centered around amino acid 35_{+8} (corresponding to AA35 in mature wildtype BMP2 and AA316 in preproBMP2). A hydrophilic substitution at this position, for example Ala →Asn, is able to eliminate this aggregation tendency; however Asn35 would also abrogate BMP type II receptor binding and thus inactivate BMP activity [39,58]. Further, the flexible N-terminus of the BMP2 growth factor domain was equipped with additional basic AAs (s. Fig. 1 B; AA 2_{+1} to 2_{+8}) to elevate solubility and concomitantly strengthen the heparin binding [35,36,59].

Biologically active BMP-2 requires the presence of a correctly folded cystine-knot; a characteristic structural motif formed by three intramolecular disulfide linkages in which two "outer" disulfide bonds form a ring that is then penetrated by a third disulfide bond. If one now figuratively pulled on the N- and C-terminal end of a cystine-knot containing protein the knot will be tied. Without a properly built cystine-knot BMP proteins are unstable and exhibit a strong propensity to irreversibly form high molecular weight aggregates. Functional analyses of BMP2 employing BMP heterodimers with individually addressed receptor binding properties revealed that simultaneous binding of two type II receptors is essential for signaling and bioactivity [78]. Similarly, binding of at least one type I receptor, whose binding epitope is formed from overlapping parts of two monomer subunits is necessary for the BMP growth factor to at least develop partial bioactivity [78]. Hence dimer formation is a prerequisite for BMP receptor activation suggesting that neither BMP monomers nor BMP aggregates do exhibit any bioactivity. While in BMPs dimerization seems to be dependent on formation of an intermolecular disulfide this assumption is not true. Although most BMPs comprise a 7th cysteine residue (which is the fourth-last cysteine in the C-terminal growth factor domain) that engages in the intermolecular disulfide, there are three examples of BMP members, i.e. GDF3, GDF9 and BMP15, that lack this particular cysteine but were reported to nevertheless form dimers [37]. In fact, in case of BMP15 and GDF9 the lack of the intermolecular disulfide is actually considered as a functional feature as it allows for the formation of BMP15/GDF9 heterodimers that have unique biological functionalities and activities even outside the cell/endoplasmic reticulum [79–81]. Hence the intermolecular disulfide bond likely stabilizes and (more importantly) fixates the BMP dimer but might not be essential for initial dimerization. Own observations however also show that monomeric BMPs have a strong tendency for aggregation and can therefore decrease protein yield during purification due to forming large protein aggregates. In accordance to this, expression in the *E. coli* strain BL21 (DE3) did not produce detectable amounts of soluble dimeric BMP2-2Hep-7M due to the reducing redox potential within the cytoplasm established through a wildtype-like glutathione and a thioredoxin pathway [82,83]. Two of the other *E. coli* strains tested, i.e. Origami™ B (DE3) and SHuffle® T7, contain loss-of-function mutations in either glutathione reductase and/or thioredoxin reductase, which regulate the two major redox potential controlling pathways in *E. coli* [84]. As additional feature the *E. coli* strain SHuffle® T7 (over) expresses the disulfide bridge isomerase C (cDsbC) into the cytosol thereby providing disulfide-isomerase activity [84]. This activity, which is normally absent in the cytoplasm and only found in limited quantities in the periplasm, can strongly facilitate formation of the native/correct disulfide-bond pattern in BMP2 [31]. The greater yield of soluble dimeric BMP2-2Hep-7M following expression in SHuffle® T7 accounts for the heterologous production of properly folded, disulfide-linked proteins. Furthermore, not only the advantageous characteristics of this *E. coli* strain enhances the chance of soluble expression of native folded BMP2 but also the hydrophilic mutations within our new generated BMP2 variant (BMP2-2Hep-7M) led to a higher amount of soluble protein. This could be proven by comparative expression of wt-BMP2* vs. BMP2-2Hep-7M (Fig. 4) in *E. coli* Shuffle® T7. Only BMP2-2Hep-7M was expressed as a soluble protein in high yield whereas the wildtype was exclusively detected in the insoluble fractions. However, BMP2-2Hep-7M will need to be examined regarding its mutations and compared to wt-BMP2 in *in vitro* and *in vivo* experiments later on. Special focus with regard to these future characterizations of BMP2-2Hep-7M for bone healing *in vitro* and *in vivo* will be given to a potential antigenicity associated with the amino acid changes that we have employed.

4.1. Protein purification

While the mutations introduced into the variant BMP2-2Hep-7M decreased the aggregation capacity observed in wildtype BMP2 the high protein concentration during purification as well as the presence of endogenous bacterial proteins can still significantly decrease protein

yield due to aggregate formation and unspecific interactions. We therefore tested supplementing the cellular lysate with L-arginine, which increased the solubility of the BMP2 variant dramatically. The L-arginine supplementation was thus used during lysis, as well as for binding and washing buffers during purification. This solubilizing effect of L-arginine was shown in various publications [85–88]. However, rising the L-arginine concentrations to 1 M impaired/attenuated the binding of BMP2-2Hep-7M to the heparin moieties on the column resin and thus caused elution of the protein from column at low ionic strength severely limiting the purification efficacy of the heparin chromatography.

Heparin, a polysulfonated, polyanionic carbohydrate can act as cation exchange chromatography column but can also function as affinity resin if the negatively charged carbohydrate can bind to specifically charged surface patches in the protein. In our design of a soluble BMP2 protein we engineered an improved heparin interaction site into the BMP2 variant. The latter allows enhanced targeting of BMP2-2Hep-7M towards the extracellular matrix *in vivo* and at the same time an enhanced flexibility regarding protein surface functionalization strategies and coupling reactions to improve implant coatings. Concerning BMP2-2Hep-7M production we achieved an efficient one-step IEC-like purification combined with affinity chromatography on heparin-Sepharose. However, several contaminating *E. coli* proteins were detected in BMP2-2Hep-7M enriched fractions. This may reflect proteins with polyanion-recognizing binding sites (e.g. RNA- and DNA-binding proteins) also found in cytoplasmic *E. coli* proteins [89].

During optimization of our purification protocol employing a heparin-Sepharose resin we tested a pH constant high-salt elution (50 mM Tris pH 5.3, 2 M NaCl) resulting in highly enriched BMP2-2Hep-7M fractions at 100% elution buffer. Tricine-SDS-PAGE analysis showed a greater than 90% purity of the monomeric and dimeric BMP2-2Hep-7M protein species eluted. However, a subsequent polishing purification step employing size exclusion chromatography (SEC) yielded a single sharp peak eluting in the void volume of the SEC-column used. Proteins from these elution fractions exhibited a high hydrodynamic radius when analyzed by DLS – supporting the idea of soluble but inactive (and non-native) BMP2-2Hep-7M-aggregates.

Purification of BMP2-2Hep-7M-dimers was optimized by eluting the BMP protein with a basic (pH 8.8) elution buffer system containing 0.5 M L-arginine and 0.5 M sodium chloride (see Table 3 and Fig. 1s) while application of the protein to the column was performed at acidic conditions (pH 5.3). Only by using this purification scheme we were able to obtain low molecular weight BMP2 proteins (see R_h, Table 3). This observation might be due to (a) a higher dimerization rate or faster intermolecular disulfide bond formation under basic conditions, stabilizing dimer formation and attenuating aggregation, (b) L-arginine as a supporting co-chaperone for solubilization of native proteins [88] and (c) lower sodium chloride concentrations for eluting the BMP2 variant from the resin corresponding to a decreased salting out effect, which is lowering hydrophobic forces possibly enhancing BMP2 aggregation. L-arginine was also shown to minimize unspecific interactions between proteins and column material and improved separation performance (Table 3) [85]. Adding urea (6 M) to selected buffers resulted in elution of proteins with medium R_h values (slightly above 10–20 nm) in a higher yield but still not in low R_h values (data not shown). This could be explained by the denaturing nature of urea at high concentrations [90–92], disaggregating high molecular weight complexes. Others explain the purification enhancement when using urea by lowered protein-protein-interactions [93] mainly due to covering [90–92].

The established expression and purification scheme for the newly designed BMP2 variant BMP2-2Hep-7M enabled an alternative soluble expression and production of a dimeric natively folded BMP2 in bacteria with reduced number of purification steps thereby saving time and cost-intensive renaturation procedures. It must be considered that only about 15–20% of the finally achieved protein yield represents the BMP2-2Hep-7M dimer while all other proteins represent mostly endogenous *E. coli* proteins (especially ribosomal proteins) and low amounts of monomeric and oligomeric BMP2-2Hep-7M (Fig. 7). Nevertheless, the actual final yield of 14.4 mg BMP2-2Hep-7M per g cell dry weight is highly promising for further up-scaling especially for soluble BMP2 expression.

5. Conclusions

This work showed a low-cost and time-saving alternative to current production of BMP2-dimer by *E. coli* by protein engineering of a more soluble designer BMP2 variant. The resulting variant BMP2-2Hep-7M could be produced by soluble expression and purification avoiding *in vitro* renaturation techniques based on inclusion bodies, which are used up to date. However, contaminating *E. coli* proteins and the remaining oligomerization property of BMP2-2Hep-7M still presents a problem and reduces the overall yield of natively folded dimeric protein. Further experiments will focus especially on reducing contaminants and decreasing oligomerization potential e.g. by co-expression of eukaryotic chaperones or further hydrophilic mutations near A35. With the data provided here, we have proven that BMP2 can be isolated from *E. coli* as a natively folded protein without the need of re-folding. Due to simple and economizing methods the presented expression and purification can be easily scaled up in relatively short time to produce large amounts of soluble BMP2-2Hep-7M dimer. Further full functional characterization – in both *in vitro* and *in vivo* – of the osteoinductive potential of this new BMP2 variant will be required to reveal its full potential.

Declaration of competing interest

The authors declare that they have no known competing financial interests or personal relationships that could have appeared to influence the work reported in this paper.

Acknowledgements

This work was supported by Westfälische Hochschule, Westphalian University of Applied Sciences August-Schmidt-Ring 10 45665 Recklinghausen Germany. The research did not receive any other specific grant from funding agencies in the public, commercial, or not-for-profit sectors.

For mass spectrometry (C.W.), we would like to acknowledge the assistance of the Core Facility BioSupraMol supported by the Deutsche Forschungsgemeinschaft (DFG).

Further scientific and experimental support: Mr. Küper (Morphoplant GmbH, 44799 Bochum, Germany; lyophilization) and Dr. Beatrix Santiago-Schübel (Forschungszentrum Jülich, ZEA-3/Building 4.8, 52425 Jülich, ESI-MS). We would also like to acknowledge Monika Brummel for ideas and scientific discussions and Sonja Niedrig (technical assistant FU Berlin) for scientific support. Graphical abstract was created using Biorender, BioRender.com, license to P.K.

Appendix A. Supplementary data

Supplementary data to this article can be found online at https://doi.org/10.1016/j.pep.2021.105918.

References

[1] M.R. Urist, Bone: formation by autoinduction, Science (New York, N.Y.) 150 (1965) 893–899.
[2] M.R. Urist, P.H. Hay, F. Dubuc, K. Buring, Osteogenetic competence, Clin. Orthop. Relat. Res. 64 (1969) 194–220.
[3] M.R. Urist, A. Mikulski, A. Lietze, Solubilized and insolubilized bone morphogenetic protein, Proc. Natl. Acad. Sci. U.S.A. 76 (1979) 1828–1832.
[4] M.R. Urist, B.F. Silverman, K. Büring, F.L. Dubuc, J.M. Rosenberg, The bone induction principle, Clin. Orthop. Relat. Res. 53 (1967) 243–283.
[5] M.R. Urist, H. Nogami, Morphogenetic substratum for differentiation of cartilage in tissue culture, Nature 225 (1970) 1051–1052.
[6] J.M. Wozney, Overview of bone morphogenetic proteins, Spine 27 (2002) S2–S8.
[7] M.F. Termaat, F.C. Den Boer, F.C. Bakker, P. Patka, H.J.T.M. Haarman, Bone morphogenetic proteins. Development and clinical efficacy in the treatment of

fractures and bone defects, the Journal of bone and joint surgery, Am. vol. 87 (2005) 1367–1378.
[8] Di Chen, M. Zhao, G.R. Mundy, Bone morphogenetic proteins, Growth Factors 22 (2004) 233–241.
[9] J. Yang, P. Shi, M. Tu, Y. Wang, M. Liu, F. Fan, M. Du, Bone morphogenetic proteins: relationship between molecular structure and their osteogenic activity, Food Sci. Human Wellness 3 (2014) 127–135.
[10] J.H. Christiansen, E.G. Coles, D.G. Wilkinson, Molecular control of neural crest formation, migration and differentiation, Curr. Opin. Cell Biol. 12 (2000) 719–724.
[11] A.H. Reddi, BMPs: from bone morphogenetic proteins to body morphogenetic proteins, Cytokine Growth Factor Rev. 16 (2005) 249–250.
[12] D.O. Wagner, C. Sieber, R. Bhushan, J.H. Börgermann, D. Graf, P. Knaus, BMPs: from bone to body morphogenetic proteins, Sci. Signal. 3 (2010) mr1.
[13] K. Ruschke, C. Hiepen, J. Becker, P. Knaus, BMPs are mediators in tissue crosstalk of the regenerating musculoskeletal system, Cell Tissue Res. 347 (2012) 521–544.
[14] T.D. Mueller, J. Nickel, Promiscuity and specificity in BMP receptor activation, FEBS Lett. 586 (2012) 1846–1859.
[15] A.C. Carreira, F.H. Lojudice, E. Halcsik, R.D. Navarro, M.C. Sogayar, J. M. Granjeiro, Bone morphogenetic proteins: facts, challenges, and future perspectives, J. Dent. Res. 93 (2014) 335–345.
[16] I. El Bialy, W. Jiskoot, M. Reza Nejadnik, Formulation, delivery and stability of bone morphogenetic proteins for effective bone regeneration, Pharmaceut. Res. 34 (2017) 1152–1170.
[17] A. Nauth, J. Ristiniemi, M.D. McKee, E.H. Schemitsch, Bone morphogenetic proteins in open fractures: past, present, and future, Injury 40 (2009) S27–S31.
[18] R.D. Welch, A.L. Jones, R.W. Bucholz, C.M. Reinert, J.S. Tjia, W.A. Pierce, J. M. Wozney, X.J. Li, Effect of recombinant human bone morphogenetic protein-2 on fracture healing in a goat tibial fracture model, J. Bone Miner. Res. : Off. J. Am. Soc. Bone Mineral Res. 13 (1998) 1483–1490.
[19] J.O. Hollinger, J.M. Schmitt, D.C. Buck, R. Shannon, S.-P. Joh, H.D. Zegzula, J. Wozney, Recombinant human bone morphogenetic protein-2 and collagen for bone regeneration, J. Biomed. Mater. Res. 43 (1998) 356–364.
[20] M. Geiger, R.H. Li, W. Friess, Collagen sponges for bone regeneration with rhBMP-2, Adv. Drug Deliv. Rev. 55 (2003) 1613–1629.
[21] Z. Dahabreh, G.M. Calori, N.K. Kanakaris, V.S. Nikolaou, P.V. Giannoudis, A cost analysis of treatment of tibial fracture nonunion by bone grafting or bone morphogenetic protein-7, Int. Orthop. 33 (2009) 1407–1414.
[22] G. Zimmermann, C. Wagner, K. Schmeckenbecher, A. Wentzensen, A. Moghaddam, Treatment of tibial shaft non-unions: bone morphogenetic proteins versus autologous bone graft, Injury 40 (2009) S50–S53.
[23] P.C. Bessa, M. Casal, R.L. Reis, Bone morphogenetic proteins in tissue engineering: the road from laboratory to clinic, part II (BMP delivery), J. Tissue Eng. Regenerative Med. 2 (2008) 81–96.
[24] A.W. James, G. LaChaud, J. Shen, G. Asatrian, V. Nguyen, X. Zhang, K. Ting, C. Soo, A review of the clinical side effects of bone morphogenetic protein-2, tissue engineering, Part B, Rev. 22 (2016) 284–297.
[25] Y. Cui, F. Jean, G. Thomas, J.L. Christian, BMP-4 is proteolytically activated by furin and/or PC6 during vertebrate embryonic development, EMBO J. 17 (1998) 4735–4743.
[26] B. Gámez, E. Rodriguez-Carballo, F. Ventura, BMP signaling in telencephalic neural cell specification and maturation, Front. Cell. Neurosci. 7 (2013) 87.
[27] D.I. Israel, J. Nove, K.M. Kerns, I.K. Moutsatsos, R.J. Kaufman, Expression and characterization of bone morphogenetic protein-2 in Chinese hamster ovary cells, Growth Factors 7 (1992) 139–150.
[28] C. Sieber, J. Kopf, C. Hiepen, P. Knaus, Recent advances in BMP receptor signaling, Cytokine Growth Factor Rev. 20 (2009) 343–355.
[29] H. Ohta, S. Wakitani, K. Tensho, H. Horiuchi, S. Wakabayashi, N. Saito, Y. Nakamura, K. Nozaki, Y. Imai, K. Takaoka, The effects of heat on the biological activity of recombinant human bone morphogenetic protein-2, J. Bone Miner. Metabol. 23 (2005) 420–425.
[30] L.F. Vallejo, U. Rinas, Folding and dimerization kinetics of bone morphogenetic protein-2, a member of the transforming growth factor-β family, FEBS J. 280 (2013) 83–92.
[31] C. Scheufler, W. Sebald, M. Hülsmeyer, Crystal structure of human bone morphogenetic protein-2 at 2.7 A resolution, J. Mol. Biol. 287 (1999) 103–115.
[32] J. Groppe, J. Greenwald, E. Wiater, J. Rodriguez-Leon, A.N. Economides, W. Kwiatkowski, M. Affolter, W.W. Vale, J.C. Izpisua Belmonte, S. Choe, Structural basis of BMP signalling inhibition by the cystine knot protein Noggin, Nature 420 (2002) 636–642.
[33] K. Nolan, T.B. Thompson, The DAN Family: Modulators of TGF-β Signaling and beyond, Protein Science : a Publication of the Protein Society, vol. 23, 2014, pp. 999–1012.
[34] S. Daopin, K.A. Piez, Y. Ogawa, D.R. Davies, Crystal structure of transforming growth factor-beta 2: an unusual fold for the superfamily, Science (New York, N.Y.) 257 (1992) 369–373.
[35] N.S. Gandhi, R.L. Mancera, Prediction of heparin binding sites in bone morphogenetic proteins (BMPs), Biochim. Biophys. Acta 1824 (2012) 1374–1381.
[36] R. Ruppert, E. Hoffmann, W. Sebald, Human bone morphogenetic protein 2 contains a heparin-binding site which modifies its biological activity, Eur. J. Biochem. 237 (1996) 295–302.
[37] A.P. Hinck, T.D. Mueller, T.A. Springer, Structural biology and evolution of the TGF-β family, Cold Spring Harbor Perspect. Biol. 8 (2016).
[38] E. Migliorini, P. Horn, T. Haraszti, S.V. Wegner, C. Hiepen, P. Knaus, R.P. Richter, E.A. Cavalcanti-Adam, Enhanced biological activity of BMP-2 bound to surface-grafted heparan sulfate, Adv. Biosys. 1 (2017), e1600041.
[39] T. Kirsch, J. Nickel, W. Sebald, BMP-2 antagonists emerge from alterations in the low-affinity binding epitope for receptor BMPR-II, EMBO J. 19 (2000) 3314–3324.
[40] E.A. Wang, V. Rosen, P. Cordes, R.M. Hewick, M.J. Kriz, D.P. Luxenberg, B. S. Sibley, J.M. Wozney, Purification and characterization of other distinct bone-inducing factors, Proc. Natl. Acad. Sci. U.S.A. 85 (1988) 9484–9488.
[41] C. Kirker-Head, Potential applications and delivery strategies for bone morphogenetic proteins, Adv. Drug Deliv. Rev. 43 (2000) 65–92.
[42] H.J. Ihm, S.-J. Yang, J.-W. Huh, S.Y. Choi, S.-W. Cho, Soluble expression and purification of synthetic human bone morphogenetic protein-2 in Escherichia coli, BMB Reports 41 (2008) 404–407.
[43] L.F. Vallejo, M. Brokelmann, S. Marten, S. Trappe, J. Cabrera-Crespo, A. Hoffmann, G. Gross, H.A. Weich, U. Rinas, Renaturation and purification of bone morphogenetic protein-2 produced as inclusion bodies in high-cell-density cultures of recombinant Escherichia coli, J. Biotechnol. 94 (2002) 185–194.
[44] Y. Maruoka, S. Oida, T. Iimura, K. Takeda, I. Asahina, S. Enomoto, S. Sasaki, Production of functional human bone morphogenetic protein-2 using a baculovirus/Sf-9 insect cell system, Biochem. Mol. Biol. Int. 35 (1995) 957–963.
[45] B. Owczarek, A. Gerszberg, K. Hnatuszko-Konka, A brief reminder of systems of production and chromatography-based recovery of recombinant protein biopharmaceuticals, BioMed Res. Int. 2019 (2019) 4216060.
[46] M. Guiotto, W. Raffoul, A.M. Hart, M.O. Riehle, P.G. Di Summa, Human platelet lysate to substitute fetal bovine serum in hMSC expansion for translational applications: a systematic review, J. Transl. Med. 18 (2020) 351.
[47] T. Yao, Y. Asayama, Animal-cell culture media: history, characteristics, and current issues, Reprod. Med. Biol. 16 (2017) 99–117.
[48] A. Eriksson, J. Burcharth, J. Rosenberg, Animal derived products may conflict with religious patients' beliefs, BMC Med. Ethics 14 (2013) 48.
[49] O. Karnieli, O.M. Friedner, J.G. Allickson, N. Zhang, S. Jung, D. Fiorentini, E. Abraham, S.S. Eaker, T.K. Yong, A. Chan, S. Griffiths, A.K. Wehn, S. Oh, A consensus introduction to serum replacements and serum-free media for cellular therapies, Cytotherapy 19 (2017) 155–169.
[50] K. Lebozec, M. Jandrot-Perrus, G. Avenard, O. Favre-Bulle, P. Billiald, Quality and cost assessment of a recombinant antibody fragment produced from mammalian, yeast and prokaryotic host cells: a case study prior to pharmaceutical development, New Biotechnol. 44 (2018) 31–40.
[51] B. Quaas, L. Burmeister, Z. Li, A. Satalov, P. Behrens, A. Hoffmann, U. Rinas, Stability and biological activity of E. coli derived soluble and precipitated bone morphogenetic protein-2, Pharmaceut. Res. 36 (2019) 184.
[52] K. Bessho, Y. Konishi, S. Kaihara, K. Fujimura, Y. Okubo, T. Iizuka, Bone induction by Escherichia coli -derived recombinant human bone morphogenetic protein-2 compared with Chinese hamster ovary cell-derived recombinant human bone morphogenetic protein-2, Br. J. Oral Maxillofac. Surg. 38 (2000) 645–649.
[53] N.R. Kübler, J.F. Reuther, G. Faller, T. Kirchner, R. Ruppert, W. Sebald, Inductive properties of recombinant human BMP-2 produced in a bacterial expression system, Int. J. Oral Maxillofac. Surg. 27 (1998) 305–309.
[54] B. Fischer, I. Sumner, P. Goodenough, Isolation, renaturation, and formation of disulfide bonds of eukaryotic proteins expressed in Escherichia coli as inclusion bodies, Biotechnol. Bioeng. 41 (1993) 3–13.
[55] S. von Einem, E. Schwarz, R. Rudolph, A novel TWO-STEP renaturation procedure for efficient production of recombinant BMP-2, Protein Expr. Purif. 73 (2010) 65–69.
[56] K.I. Piatkov, T.T.M. Vu, C.-S. Hwang, A. Varshavsky, Formyl-methionine as a degradation signal at the N-termini of bacterial proteins, Microbial Cell (Graz, Austria) 2 (2015) 376–393.
[57] O. Conchillo-Solé, N.S. de Groot, F.X. Avilés, J. Vendrell, X. Daura, S. Ventura, AGGRESCAN: a server for the prediction and evaluation of "hot spots" of aggregation in polypeptides, BMC Bioinf. 8 (2007) 65.
[58] W. Sebald, J. Nickel, J.-L. Zhang, T.D. Mueller, Molecular recognition in bone morphogenetic protein (BMP)/receptor interaction, Biol. Chem. 385 (2004) 697–710.
[59] R.A.A. Smith, S. Murali, B. Rai, X. Lu, Z.X.H. Lim, J.J.L. Lee, V. Nurcombe, S. M. Cool, Minimum structural requirements for BMP-2-binding of heparin oligosaccharides, Biomaterials 184 (2018) 41–55.
[60] K.K. Würzler, J. Emmert, F. Eichelsbacher, N.R. Kübler, W. Sebald, J.F. Reuther, Evaluation der osteoinduktiven Potenz von gentechnisch modifizierten BMP-2-Varianten, Mund-, Kiefer- und Gesichtschirurgie, MKG 8 (2004) 83–92.
[61] R. Depprich, J. Handschel, W. Sebald, N.R. Kübler, K.K. Würzler, Vergleich der osteogenen Potenz gentechnisch modifizierter BMP, Mund-, Kiefer- und Gesichtschirurgie, MKG 9 (2005) 363–368.
[62] J.A. Cuff, G.J. Barton, Application of multiple sequence alignment profiles to improve protein secondary structure prediction, Proteins 40 (2000) 502–511.
[63] H. Schägger, Tricine-SDS-PAGE, Nat. Protoc. 1 (2006) 16–22.
[64] N. Dyballa, S. Metzger, Fast and sensitive colloidal coomassie G-250 staining for proteins in polyacrylamide gels, J. Vis. Exp. (2009), https://doi.org/10.3791/1431.
[65] N.R. Kübler, K.K. Würzler, J.F. Reuther, E. Sieber, T. Kirchner, W. Sebald, Einfluss unterschiedlicher Faktoren auf die knochenbildenden Eigenschaften von rekombinanten BMPs, Mund-, Kiefer- Gesichtschirurgie : MKG 4 (Suppl 2) (2000) S465–S469.
[66] N.R. Kübler, K. Würzler, J.F. Reuther, G. Faller, E. Sieber, T. Kirchner, W. Sebald, EHBMP-2. Erstes BMP-Analog mit osteoinduktiven Eigenschaften, Mund-, Kiefer-Gesichtschirurgie : MKG 3 (Suppl 1) (1999) S134–S139.
[67] L.J. McGuffin, K. Bryson, D.T. Jones, The PSIPRED protein structure prediction server, Bioinformatics 16 (2000) 404–405.
[68] D.W.A. Buchan, D.T. Jones, The PSIPRED protein analysis workbench: 20 years on, Nucleic Acids Res. 47 (2019) W402–W407.

[69] D.T. Jones, Protein secondary structure prediction based on position-specific scoring matrices, J. Mol. Biol. 292 (1999) 195–202.
[70] C.H. Schein, M.H.M. Noteborn, formation of soluble recombinant proteins in Escherichia coli is favored by lower growth temperature, Nat. Biotechnol. 6 (1988) 291–294.
[71] A. Vera, N. González-Montalbán, A. Arís, A. Villaverde, The conformational quality of insoluble recombinant proteins is enhanced at low growth temperatures, Biotechnol. Bioeng. 96 (2007) 1101–1106.
[72] T.A. Bewley, C.H. Li, The reduction of protein disulfide bonds in the absence of denaturants, Int. J. Protein Res. 1 (1969) 117–124.
[73] A.P.J. Middelberg, Preparative protein refolding, Trends Biotechnol. 20 (2002) 437–443.
[74] N.E. Sharapova, A.P. Kotnova, Z.M. Galushkina, N.V. Lavrova, N.N. Poletaeva, A. E. Tukhvatulin, A.S. Semikhin, A.V. Gromov, L.A. Soboleva, A.S. Ershova, V. V. Zaitsev, O.V. Sergienko, V.G. Lunin, A.S. Karyagina, Production of the recombinant human bone morphogenetic protein-2 in Escherichia coli and testing of its biological activity in vitro and in vivo, Mol. Biol. 44 (2010) 923–930.
[75] H. Zhang, J. Wu, Y. Zhang, N. Fu, J. Wang, S. Zhao, Optimized procedure for expression and renaturation of recombinant human bone morphogenetic protein-2 at high protein concentrations, Mol. Biol. Rep. 37 (2010) 3089–3095.
[76] Y. Zhang, Y. Ma, M. Yang, S. Min, J. Yao, L. Zhu, Expression, purification, and refolding of a recombinant human bone morphogenetic protein 2 in vitro, Protein Expr. Purif. 75 (2011) 155–160.
[77] F. Hillger, G. Herr, R. Rudolph, E. Schwarz, Biophysical comparison of BMP-2, ProBMP-2, and the free pro-peptide reveals stabilization of the pro-peptide by the mature growth factor, J. Biol. Chem. 280 (2005) 14974–14980.
[78] P. Knaus, W. Sebald, Cooperativity of binding epitopes and receptor chains in the BMP/TGFbeta superfamily, Biol. Chem. 382 (2001) 1189–1195.
[79] D.A. Heath, J.L. Pitman, K.P. McNatty, Molecular forms of ruminant BMP15 and GDF9 and putative interactions with receptors, Reproduction 154 (2017) 521–534.
[80] D.G. Mottershead, S. Sugimura, S.L. Al-Musawi, J.-J. Li, D. Richani, M.A. White, G. A. Martin, A.P. Trotta, L.J. Ritter, J. Shi, T.D. Mueller, C.A. Harrison, R.B. Gilchrist, Cumulin, an oocyte-secreted heterodimer of the transforming growth factor-β family, is a potent activator of granulosa cells and improves oocyte quality, J. Biol. Chem. 290 (2015) 24007–24020.
[81] D.G. Mottershead, C.A. Harrison, T.D. Mueller, P.G. Stanton, R.B. Gilchrist, K. P. McNatty, Growth differentiation factor 9:bone morphogenetic protein 15 (GDF9: BMP15) synergism and protein heterodimerization, Proc. Natl. Acad. Sci. U.S.A. 110 (2013) E2257.
[82] P.H. Bessette, F. Aslund, J. Beckwith, G. Georgiou, Efficient folding of proteins with multiple disulfide bonds in the Escherichia coli cytoplasm, Proc. Natl. Acad. Sci. U. S.A. 96 (1999) 13703–13708.
[83] W.A. Prinz, F. Aslund, A. Holmgren, J. Beckwith, The role of the thioredoxin and glutaredoxin pathways in reducing protein disulfide bonds in the Escherichia coli cytoplasm, J. Biol. Chem. 272 (1997) 15661–15667.
[84] J. Lobstein, C.A. Emrich, C. Jeans, M. Faulkner, P. Riggs, M. Berkmen, SHuffle, a novel Escherichia coli protein expression strain capable of correctly folding disulfide bonded proteins in its cytoplasm, Microb. Cell Factories 11 (2012) 56.
[85] T. Arakawa, D. Ejima, K. Tsumoto, N. Obeyama, Y. Tanaka, Y. Kita, S.N. Timasheff, Suppression of protein interactions by arginine: a proposed mechanism of the arginine effects, Biophys. Chem. 127 (2007) 1–8.
[86] J. Chen, Y. Liu, Y. Wang, H. Ding, Z. Su, Different effects of L-arginine on protein refolding: suppressing aggregates of hydrophobic interaction, not covalent binding, Biotechnol. Prog. 24 (2008) 1365–1372.
[87] B.M. Baynes, D.I.C. Wang, B.L. Trout, Role of arginine in the stabilization of proteins against aggregation, Biochemistry 44 (2005) 4919–4925.
[88] K. Tsumoto, M. Umetsu, I. Kumagai, D. Ejima, J.S. Philo, T. Arakawa, Role of arginine in protein refolding, solubilization, and purification, Biotechnol. Prog. 20 (2004) 1301–1308.
[89] K. Robison, A.M. McGuire, G.M. Church, A comprehensive library of DNA-binding site matrices for 55 proteins applied to the complete Escherichia coli K-12 genome, J. Mol. Biol. 284 (1998) 241–254.
[90] D.R. Canchi, D. Paschek, A.E. García, Equilibrium study of protein denaturation by urea, J. Am. Chem. Soc. 132 (2010) 2338–2344.
[91] M.C. Stumpe, H. Grubmüller, Interaction of urea with amino acids: implications for urea-induced protein denaturation, J. Am. Chem. Soc. 129 (2007) 16126–16131.
[92] Q. Zou, S.M. Habermann-Rottinghaus, K.P. Murphy, Urea effects on protein stability: hydrogen bonding and the hydrophobic effect, Proteins 31 (1998) 107–115.
[93] F. Khademi, A. Mostafaie, Effect of urea on protein separation by ion-exchange chromatography, J. Biochem. 147 (2010) 735–741.